Science of the Total Environment 718 (2020) 137374

Contents lists available at ScienceDirect

Science of the Total Environment

journal homepage: www.elsevier.com/locate/scitotenv

Monitoring dissolved organic carbon by combining Landsat-8 and Sentinel-2 satellites: Case study in Saginaw River estuary, Lake Huron

Jiang Chen [a,b], Weining Zhu [b,*], Yong Q. Tian [c], Qian Yu [d]

[a] School of Remote Sensing and Information Engineering, Wuhan University, Hubei, China
[b] Ocean College, Zhejiang University, Zhejiang, China
[c] Institute for Great Lakes Research, Department of Geography, Central Michigan University, MI, USA
[d] Department of Geosciences, University of Massachusetts - Amherst, MA, USA

HIGHLIGHTS

- Landsat-8 and Sentinel-2 DOC models showed acceptable accuracy.
- Landsat-8 and Sentinel-2 DOC estimates were consistent within 4.9%.
- Monthly spatiotemporal variations of DOC in Lake Huron were observed.
- DOC concentrations were significantly influenced by the riverine discharge.

GRAPHICAL ABSTRACT

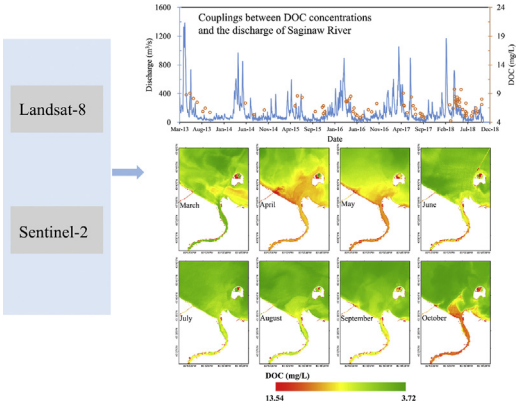

ARTICLE INFO

Article history:
Received 3 December 2019
Received in revised form 19 January 2020
Accepted 15 February 2020
Available online 17 February 2020

Editor: Christian Herrera

Keywords:
Dissolved organic carbon (DOC)
Landsat-8
Sentinel-2
Lake Huron
Remote sensing

ABSTRACT

Dissolved organic carbon (DOC) in aquatic environments is an important cycled pool of organic matter on the Earth. Satellite remote sensing provides a useful tool to determine spatiotemporal distribution of water quality parameters. Previous DOC remote sensing studies in inland water suffered from either low spatial resolution or low temporal frequency. In this study, we evaluated the potential of jointly using Landsat-8 and Sentinel-2 with high spatial resolution to estimate DOC concentrations in Saginaw River plume regions of Lake Huron. Firstly, CDOM (colored dissolved organic matter) was estimated from images using the known models and then DOC can be derived in terms of the good correlations between DOC and CDOM. The results show that Landsat-8 and Sentinel-2 had acceptable accuracy and good consistency in DOC estimation so that jointly using them can improve the observation frequency. In different seasons from 2013 to 2018, DOC was typically higher in spring and autumn but lower in summer. Monthly spatiotemporal variations of DOC in 2018 were also observed. The image-derived DOC spatiotemporal variations show that DOC was covaried with Saginaw River discharge ($r = 0.82$) and also weakly and negatively correlated with water temperature ($r = -0.6$). This study demonstrated that using Landsat-8 and Sentinel-2 together can offer the potential applications for monitoring DOC and water quality dynamic in complex inland water.

* Corresponding author.
E-mail address: zhuwn@zju.edu.cn (W. Zhu).

https://doi.org/10.1016/j.scitotenv.2020.137374
0048-9697/

1. Introduction

Dissolved organic carbon (DOC), a major fraction of dissolved organic matter (DOM) in aquatic environment, is an important cycled pool of organic matter on the Earth, accounting for 20% of the global organic carbon (Siegenthaler and Sarmiento, 1993). DOC plays a significant role in carbon cycling and climate change (Coble, 1996, 2007), and can be applied to monitor the amount of carbon storage in aquatic environments (Griffin et al., 2011; Griffin et al., 2018b). The DOC cycling in inland water is characterized by multiple terrigenous sources and mixing biological, physical, and photochemical processes (Miller and Moran, 1997; Bauer et al., 2013). In general, dissolved organic components in water are products of decomposition processes from the live or dead planktons such as macrophyte and algae (Coble, 2007). In addition, a large number of terrigenous DOC is also transported into water through river and groundwater discharge (Butman et al., 2016), making aquatic DOC concentrations even higher (Findley, 2003; Pacheco et al., 2014). Precipitation and surface runoff also carry DOC from the watershed soil organic carbon pool to lakes, estuaries and coasts (Godin et al., 2017). The increased DOC concentrations may have considerable impacts on aquatic environment, for example, high DOC abundance will affect the color of natural waters, and then adversely influence primary production by preventing the solar radiation from propagating to the ecosystem in deeper water (Bricaud et al., 1981; Coble, 2007; Joshi and D'Sa, 2015). Previous studies have demonstrated that most inland waters contain supersaturated CO_2 in their water-air interface (Tranvik et al., 2009), meaning that abundant aquatic DOC is releasing non-negligible CO_2 into atmosphere (Coble, 2007). Thus, monitoring DOC provides an effective approach to observe and understand aquatic environment and climate change.

Inland waters including streams, lakes, and wetlands only account a small proportion to the Earth's surface (Verpoorter et al., 2014), but these aquatic ecosystems act as an important role in regional and global carbon cycling (Tranvik et al., 2009). Terrestrial carbon received by inland waters was approximately 1.9 Pg every year, of which 41.11% was released to the atmosphere, 10.53% was deposited in sediments, and the remaining was transported to the ocean (Cole et al., 2007). In recent decades, one has more interest in investigating spatiotemporal distributions of DOC (Miller and Moran, 1997; Cole et al., 2007; Bauer et al., 2013; Griffin et al., 2018b). However, the traditional field-based measurement can only make a discrete observation based on limited water samples rather than a large-scope observation on the whole study area (Kutser, 2012; Joshi and D'Sa, 2015). Instead, satellite remote sensing provides a useful tool to determine spatiotemporal distributions of DOC.

Water quality remote sensing is based on the theory of radiative transfer that AOPs (apparent optical properties) observed by satellite sensors are determined by water's IOPs (inherent optical properties) (Pan et al., 2014; Mouw et al., 2015; Palmer et al., 2015). The colored dissolved organic matter (CDOM) is the optically-active fraction of DOC. CDOM has strong absorptions at the UV and short wavelengths, so that it has significant impact on underwater light field and then the satellite-observed spectra (Kirk, 1994). Many remote sensing studies of CDOM in various waters such as open seas, inland lakes, estuarine and coastal regions have been reported (Cardille et al., 2013; Zhu et al., 2013; Cao and Miller, 2015; Chen et al., 2017a; Cao et al., 2018; Li et al., 2018; Xu et al., 2018). It is known that there are good correlations between DOC and CDOM, so DOC can be remotely estimated through two steps: at first, developing a model to accurately retrieve CDOM, and then estimating DOC using the relationship between DOC and CDOM. Some satellites such as MODIS (Moderate Resolution Imaging Spectroradiometer) was used to estimate DOC in Great Lakes (Shuchman et al., 2013) and Moreton Bay (Cherukuru et al., 2016), and MEIRS (Medium Resolution Imaging Spectrometer) was used in two lakes in Sweden (Kutser et al., 2015) and different coastal and estuarine regions in North America (Cao et al., 2018). Tehrani et al. (2013) comprehensively evaluated the empirical algorithms for estimating DOC in the northern Gulf of Mexico using SeaWiFS (Sea-viewing Wide Field-of-view Sensor), MODIS, and MERIS and achieved satisfactory results. However, the spatial resolution of these satellites is not suitable for small-size inland waters such as rivers and lakes. With higher spatial resolution in 30 m, Landsat series satellites are also important tools for earth observation. Griffin et al. (2011) used Landsat-5 and Landsat-7 to estimate DOC in Kolyma River and its major tributaries and found the strong interannual variability of DOC, and they also used Landsat-5 and Landsat-7 to estimate DOC in some Arctic rivers (Griffin et al., 2018a). Liu et al. (2019) used the historical Landsat-5 data to estimate multi-decadal DOC spatiotemporal trends. However, Landsat-5 was officially decommissioned on June 5, 2013, and Landsat-7 was also with the problem that its SLC (The Scan Line Corrector) has not worked since May 31, 2003, making there are invalid gaps in Landsat-7 images.

In this study, we focused on two newly launched satellites Landsat-8 and Sentinel-2 which are with high spatial resolution 10–60 m and improved signal-to-noise ratio. Many studies have successfully used single Landsat-8 or Sentinel-2 for retrieval of CDOM (Alcântara et al., 2016; Olmanson et al., 2016; Slonecker et al., 2016; Toming et al., 2016; Chen et al., 2017a; Chen et al., 2017; Xu et al., 2017; Li et al., 2018), but there are few studies using the two popular satellites to estimate DOC distributions in inland water. A potential shortcoming of Landsat-8 is that it has a relatively long revisit time of 16 days, and once an image was heavily covered by cloud or cirrus, the observation frequency on a region of interest may be 32 days or even longer. Nevertheless, many studies have used Landsat-8 for water quality observation and driving factor analysis (Qiu et al., 2016; Zheng et al., 2016; Li et al., 2017; Li et al., 2017b; Li et al., 2018; Ren et al., 2018; Luis et al., 2019), and they also suggested that the observation and analysis might be improved if more Landsat-8-like data can be used to enhance the temporal frequency. Therefore, in this study we jointly used the Sentinel-2 satellite with high revisit time (5 days). If combining Landsat-8 and Sentinel-2, the median revisit time ranges from 14 min to 7 days and the average time is 2.9 days (Li and Roy, 2017). Although DOC/CDOM concentration is temporally more stable than the other water quality parameters such as chlorophyll-a, suspended particulate matter, and Secchi depth, the watershed precipitation and then the changes of discharge may also dramatically affect DOC/CDOM concentrations within a short time (Chen et al., 2018; Li et al., 2018; Zhao et al., 2018). Therefore, with the temporal resolution being improved, the combination of Landsat-8 and Sentinel-2 still has great advantages for monitoring DOC spatiotemporal variations in complex inland water.

The objectives of this study are to: (1) evaluate the applicability of Landsat-8 and Sentinel-2 for estimating DOC in inland water; (2) examine the consistency of the two satellites in retrieving DOC; (3) investigate the seasonal patterns of DOC using the developed retrieval models; and (4) map monthly DOC distributions and study its driving forces by combining Landsat-8 and Sentinel-2 data.

2. Data and methods

2.1. Study site

The Saginaw River and Kawkawlin River plume regions in Saginaw Bay, Lake Huron, is the study site for field water and spectrum samplings (Fig. 1). There are two rivers, Kawkawlin River and Saginaw River, flow into the Saginaw Bay. The Kawkawlin River is relatively small, with length 28.2 km and watershed area 647 km^2, while the Saginaw River is longer (36 km) and with a much larger watershed area 22,260 km^2. The land use and land cover of their watersheds are basically cropland for agriculture as well as some urban areas such as Bay City, Saginaw, and Midland. The Saginaw River usually looks more turbid than the Kawkawlin River, while because of the high-concentration CDOM, the color of Kawkawlin's water looks much darker than the Saginaw. The Saginaw Bay and its rivers provide important

water resources for drinking, irrigation, fishing, navigation, and etc. The residents and regulators in Saginaw, Midland, and Bay City always have great concerns on water quality of the bay and rivers, and hence we were motivated to monitor CDOM and DOC in the study site.

2.2. Field sampling and laboratory measurements

Three field sampling cruises were conducted in the study site on May 10 and October 18, 2012, and May 7, 2013, and 41 water samples were collected by amber Nalgene bottles, see Fig. 1. In cruises, all samples were immediately stored in a cooler to reduce the decomposition of organic matter, and then were sent to the laboratory for CDOM and DOC measurement at the same day or next day.

The above-surface spectra (400–800 nm), including the downwelling irradiance (E_d), water leaving radiance (L_t), and sky radiance (L_i), were measured using the HyperSAS (Hyperspectral Surface Acquisition System, Satlantic Inc.) and HyperOCR (Hyperspectral Ocean Color Radiometer). The viewing geometry of instruments was followed HyperSAS manual and NASA's protocol. The R_{rs}, remote sensing reflectance, was then calculated by

$$R_{rs} = \frac{L_t - \rho L_i}{E_d} \quad (1)$$

where ρ, the water surface reflectance factor accounting for the proportion of surface-reflected sky radiance, was set to 0.028 according to instrument manual and Mobley (1999). All spectra were measured between 10 A.M. and 2 P.M. with no cloud and wind speed 2–4 m/s.

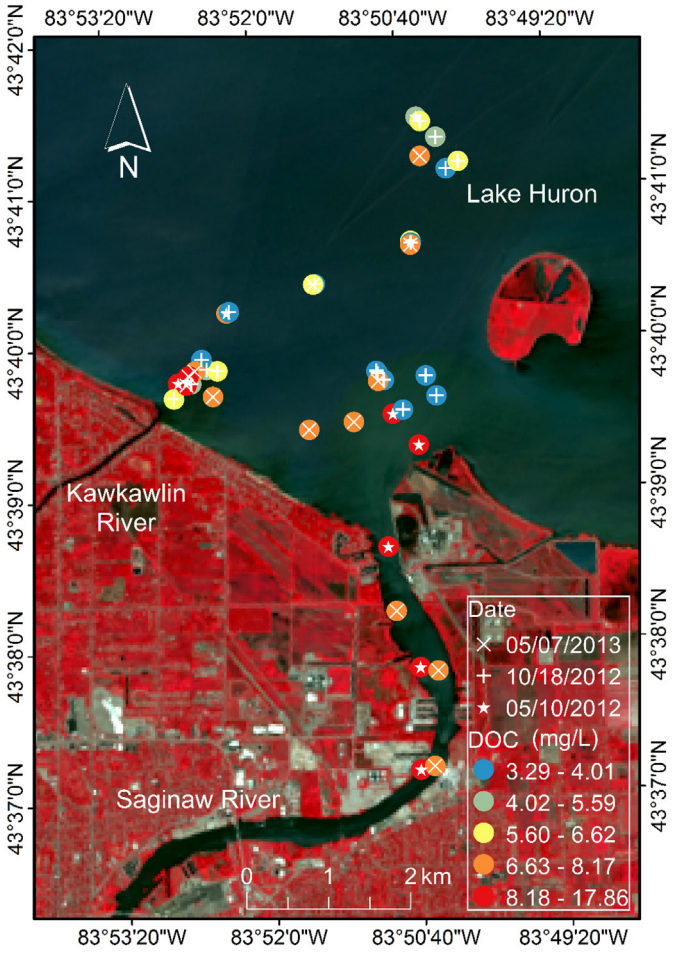

Fig. 1. Study site and sampling map: the portion of a Landsat-8 image (acquired on May 1, 2013) covering the Kawkawlin River and Saginaw River plume regions of Lake Huron.

To minimize the measurement uncertainty, each spectrum (E_d, L_t, and L_i) were measured at least 20 times at each sampling location, and then the median one was used to calculate the R_{rs}.

In laboratory, water samples were filtered by GF/F glass microfiber membrane (0.70 μm) for CDOM measurements. The absorption coefficients of CDOM (a_{CDOM}) between 200 and 800 nm were measured by a Cray-60 spectroradiometer with Milli-Q water as a baseline correction, following the below equation

$$a_{CDOM} = \frac{\ln(10) \times A(\lambda)}{L} \quad (2)$$

where $A(\lambda)$ is the optical absorbance of CDOM measured by Cary-60, and L is the cuvette path-length in meters (0.01 m in this study). The absorption coefficient at 440 nm, namely $a_{CDOM}(440)$, is usually used as the proxy of CDOM concentration (Kirk, 1994; Kutser, 2012; Zhu et al., 2013; Cao et al., 2018). DOC concentration was measured using a Shimadzu TOC-V analyzer. When 50 μL injections of water samples were combusted at 800 °C, the sample DOC concentration can be calculated from the resultant CO_2 measured with a non-dispersive infrared detector.

2.3. Image preprocessing of Landsat-8 and Sentinel-2

Atmospheric correction is a necessary image processing for remotely estimating DOC (Zheng et al., 2016; Li et al., 2018). NASA and USGS have made Landsat-8 surface reflectance (SR) Level-2 products publicly available, which can be requested and downloaded from their official websites. Recent studies have demonstrated that Landsat-8 SR products are applicable for deriving water quality parameters in complex waters (Griffin et al., 2018a; Echavarría-Caballero et al., 2019; Kuhn et al., 2019; Gomes et al., 2020). Sentinel-2 Level-1 raw products can be downloaded from ESA's website, and ESA has developed an atmospheric correction algorithm Sen2Cor to derive Sentinel-2 SR data from its Level-1 image. Some studies show that Sen2Cor is accurate to estimate Sentinel-2 SR data for water quality remote sensing modeling (Toming et al., 2016; Chen et al., 2017; Casal et al., 2019; Sòria-Perpinyà et al., 2020). Then R_{rs} can be further computed from SR with the help of the well-known water radiative transfer model, Hydrolight. The two variables including sky radiance reflected upward by the water surface at the viewing geometry and downwelling irradiance were estimated by the Hydrolight. In order to compute the two variables, some parameters, including wind speed, cloud cover, solar zenith angle, and image acquisition location and date, need to be input into Hydrolight. These parameters can be obtained from either National Climatic Data Center or image metadata. The rest input parameters, such as water color components or water depth, were set by their defaults because they are not linked to water surface reflectance. More details can be seen in (Chen et al., 2017a) and (Zhu and Yu, 2013).

In this study we processed 38 Landsat-8 and 36 Sentinel-2 cloud-free images from April 2013 to December 2018, in which most of images in winter (from Dec. to Feb.) are with poor quality since water was frozen (Chen et al., 2018; Li et al., 2018). The Landsat-8 image on May 1, 2013 was used to evaluate DOC model's performance because this day was close to the date of our field measurement on May 7, 2013. The four Landsat-8 and Sentinel-2 images on April 23, 2016 and October 22, 2018 were used to evaluate the consistency of Landsat-8 and Sentinel-2 for estimating DOC concentration.

2.4. Developing and evaluating DOC Landsat-8/Sentinel-2 models

Previous studies have developed accurate Landsat-8 and Sentinel-2 CDOM retrieval models in Saginaw Bay, Lake Huron (Chen et al., 2017a; Chen et al., 2017). The Landsat-8 CDOM model is $a_{CDOM}(440) = 40.75e^{-2.463x}$, $x = R_{rs}(\text{OLI3})/R_{rs}(\text{OLI4})$, with accuracy $R^2 = 0.829$ and RMSE $= 0.863\ m^{-1}$, and OLI3 and OLI4 are band 3 (green,

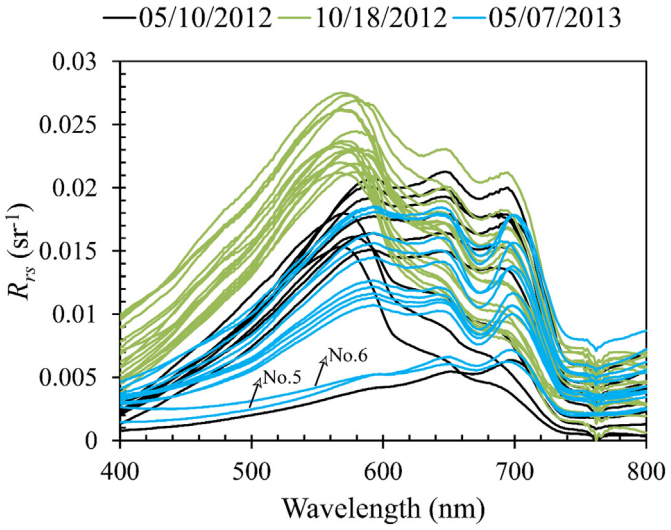

Fig. 2. Field measured above-surface spectra (R_{rs}).

561 nm) and band 4 (red, 655 nm) of Landsat-8, respectively. The Sentinel-2 CDOM model is $a_{CDOM}(440) = 28.966e^{-2.015x}$, $x = R_{rs}(MSI3)/R_{rs}(MSI4)$, with accuracy $R^2 = 0.832$ and RMSE = 0.859 m^{-1}, and MSI3 and MSI4 are band 3 (green, 560 nm) and band 4 (red, 664 nm) of Sentinel-2, respectively. In this study, we do not develop new CDOM retrieval models but used the above two models, and then model the correlations between DOC and CDOM, aiming to estimate DOC from the image-derived CDOM.

Field measured R_{rs} were used to simulate the bands of Landsat-8 and Sentinel-2 according to their spectral response functions (SRF). The SRFs were obtained from the official websites of NASA and ESA. The simulation was conducted by

$$R_{b(i)} = \frac{\int_{\lambda_{min}}^{\lambda_{max}} SRF(\lambda) R_{rs}(\lambda) d\lambda}{\int_{\lambda_{min}}^{\lambda_{max}} SRF(\lambda) d\lambda} \quad (3)$$

where $R_{b(i)}$ is the R_{rs} for the i-th band of Landsat-8 or Sentinel-2, λ_{min} and λ_{max} are the minimum and maximum wavelengths of the i-th band, and $SRF(\lambda)$ is the relative spectral response for the i-th band at wavelength λ. In this study, the performances of Landsat-8 and Sentinel-2 DOC retrieval models were evaluated using both of simulated spectra and real image. The model evaluation statistics include coefficient of determination (R^2), root mean square error (RMSE), and relative root mean square error (RRMSE), and the Pearson correlation analysis was used to determine the correlations between two variables such as DOC and discharge. After the DOC Landsat-8/Sentinel-2 models were carefully evaluated and consistency-checked, these models were then applied to 74 Landsat-8 and Sentinel-2images acquired from April 2013 to December 2018. Meanwhile, monthly spatiotemporal distributions of DOC in Saginaw River estuary in 2018 were also mapped and analyzed.

3. Results and discussion

3.1. Field measured spectra, DOC and CDOM variations

The field measured R_{rs} are shown in Fig. 2, showing the typical spectral signatures of complex inland freshwater (Toming et al., 2016; Zhang et al., 2016; Xu et al., 2018). The reflectance peaks at about 570 nm (Fig. 2) may be caused by the combinative effect of minimal absorption of algal pigments and scattering of non-algal particles (Gurlin et al., 2011). The reflectance troughs at approximately 670 nm (red band) may be caused by the maximum absorption of chlorophyll-a. The local reflectance peaks at about 700 nm were related to the minimum absorption of algal pigments and pure water. Most of samples were with high $R_{rs} > 0.01$ sr^{-1}, especially within wavelengths 500–700 nm (green and red bands). These high-R_{rs} samples were from the lake water in Saginaw River estuary and open Lake Huron areas, while a few samples, e.g., No. 5 and No. 6 in Fig. 2, were with very low reflectance. These low-R_{rs} samples were found in the small plume region of the Kawkawlin River, where the CDOM concentrations are very high (> 8 m^{-1}), making the water looks very dark, and hence leading the water-leaving radiance to be very low. Other spectral features connected to DOC/CDOM variations can refer to our previous study (Zhu et al., 2014).

The field measured DOC and $a_{CDOM}(440)$ on May 10, 2012 were with ranges of 5.42–17.86 mg/L (mean 9.92 mg/L) and 0.73–8.46 m^{-1} (mean 3.39 m^{-1}), on Oct 18, 2012, they were decreased to 3.29–5.96 mg/L (mean 4.44 mg/L) and 0.11–2.06 m^{-1} (mean 0.75 m^{-1}), and on May

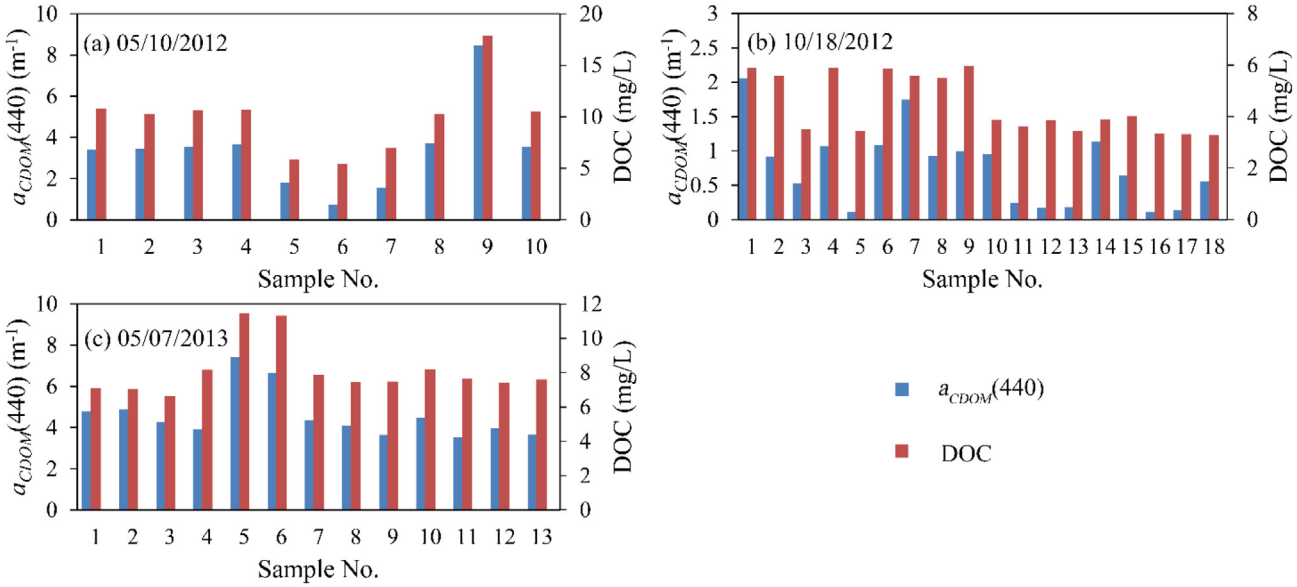

Fig. 3. The measured $a_{CDOM}(440)$ and DOC concentrations in three sampling cruises: (a) May 10, 2012, (b) Oct. 18, 2012, and (c) May 7, 2013.

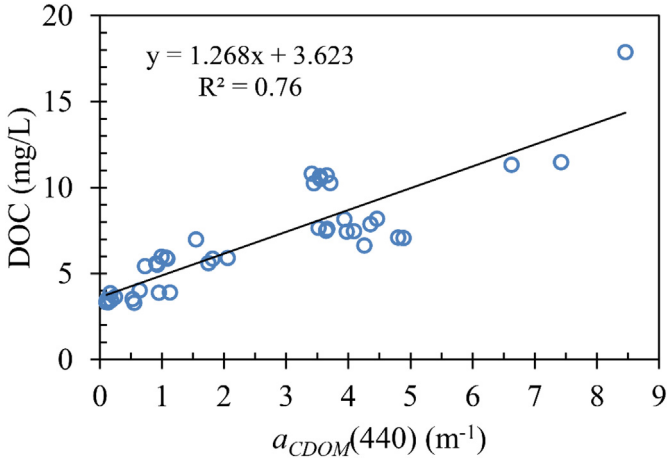

Fig. 4. Relationship between the measured $a_{CDOM}(440)$ and DOC.

7, 2013, they turned to be 6.62–11.47 mg/L (mean 8.1 mg/L) and 3.52–7.43 m^{-1} (mean 4.59 m^{-1}), respectively, see Fig. 3. Some studies have reported that snow-melting processes can boost the releasing of organic matter from soil to water, triggering the significant seasonal DOC/CDOM variations between the early May and the middle of October (Huang and Chen, 2009). For all three cruises, the sampled DOC ranged from 3.29 to 17.86 mg/L with the mean 6.94 mg/L and CV (the coefficient of variation) 44.35%, demonstrating the large variations of DOC in study area.

It is known that CDOM can be used as the indicator of DOC in many inland waters (Griffin et al., 2011; Shuchman et al., 2013; Zhu et al., 2014; Griffin et al., 2018a; Liu et al., 2019). In our study area, the results (see Fig. 4) show that there were good correlations ($R^2 = 0.76$, n = 41) between DOC and $a_{CDOM}(440)$, so the model used to estimate DOC from $a_{CDOM}(440)$ was then established by

$$DOC = 1.268a_{CDOM}(440) + 3.623 \quad (4)$$

3.2. Model performance based on simulated bands of Landsat-8 and Sentinel-2

Based on the known Landsat-8/Sentinel-2 CDOM models (see Section 2.4) and Eq. (4), DOC can be then estimated from the simulated

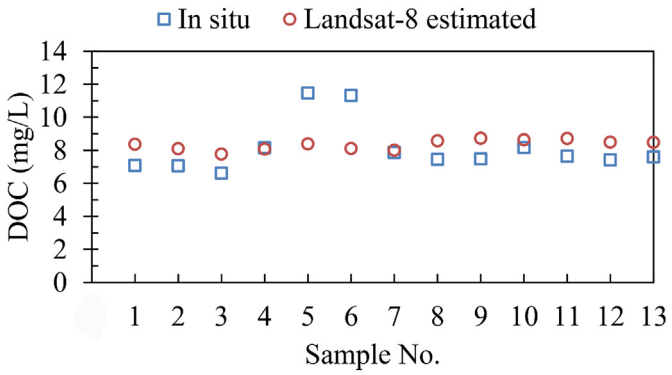

Fig. 6. Comparison between field measured DOC and Landsat-8 estimated DOC.

Landsat-8 and Sentinel-2 Bands. Fig. 5 shows the validation results of DOC retrieving. For Landsat-8 model, DOC estimations were with good accuracy $R^2 = 0.86$, RMSE = 1.13, and RRMSE = 16.28% (Fig. 5(a)). The Sentinel-2 DOC model shown the similar accuracy as the Landsat-8 DOC model with $R^2 = 0.78$, RMSE = 1.41 mg/L, and RRMSE = 20.32% (Fig. 5(b)). These validation results demonstrated that Landsat-8 and Sentinel-2 spectra and the proposed models can be used to estimate DOC concentration in the study site with acceptable accuracy.

3.3. Model application in Landsat-8 and Sentinel-2 images

Beside the simulated spectra, we also used the image-obtained spectra to test our models. The image spectra were obtained from the Landsat-8 image acquired on May 1, 2013, and the image-derived DOC were compared with the ground true DOC obtained on May 7, 2013. Although there was a 6-day gap between the field sampling and satellite passing, according to many previous studies (Griffin et al., 2011; Tebbs et al., 2013; Montanher et al., 2014; Sun et al., 2015; Lee et al., 2016; Boucher et al., 2018), the gap is still allowed for remote sensing validation, because, during the 6 days, (1) there were no dramatic weather changes such as rainfall, strong winds, and significant temperature drops; and (2) there were also no human activities such as river channel and lakeshore construction works. Moreover, recent studies have demonstrated that Landsat-8 SR products are applicable for deriving water quality parameters in complex waters (Griffin et al.,

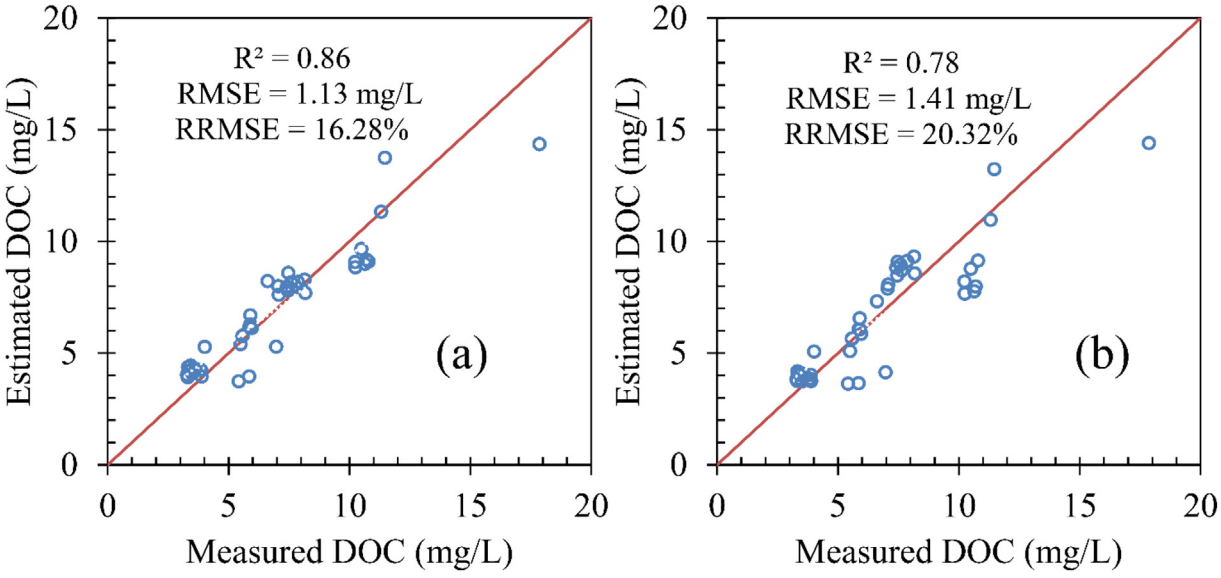

Fig. 5. Field measured DOC versus estimated DOC based on CDOM-DOC relationship and satellite-estimated CDOM for (a) Landsat-8 model and (b) Sentinel-2 model.

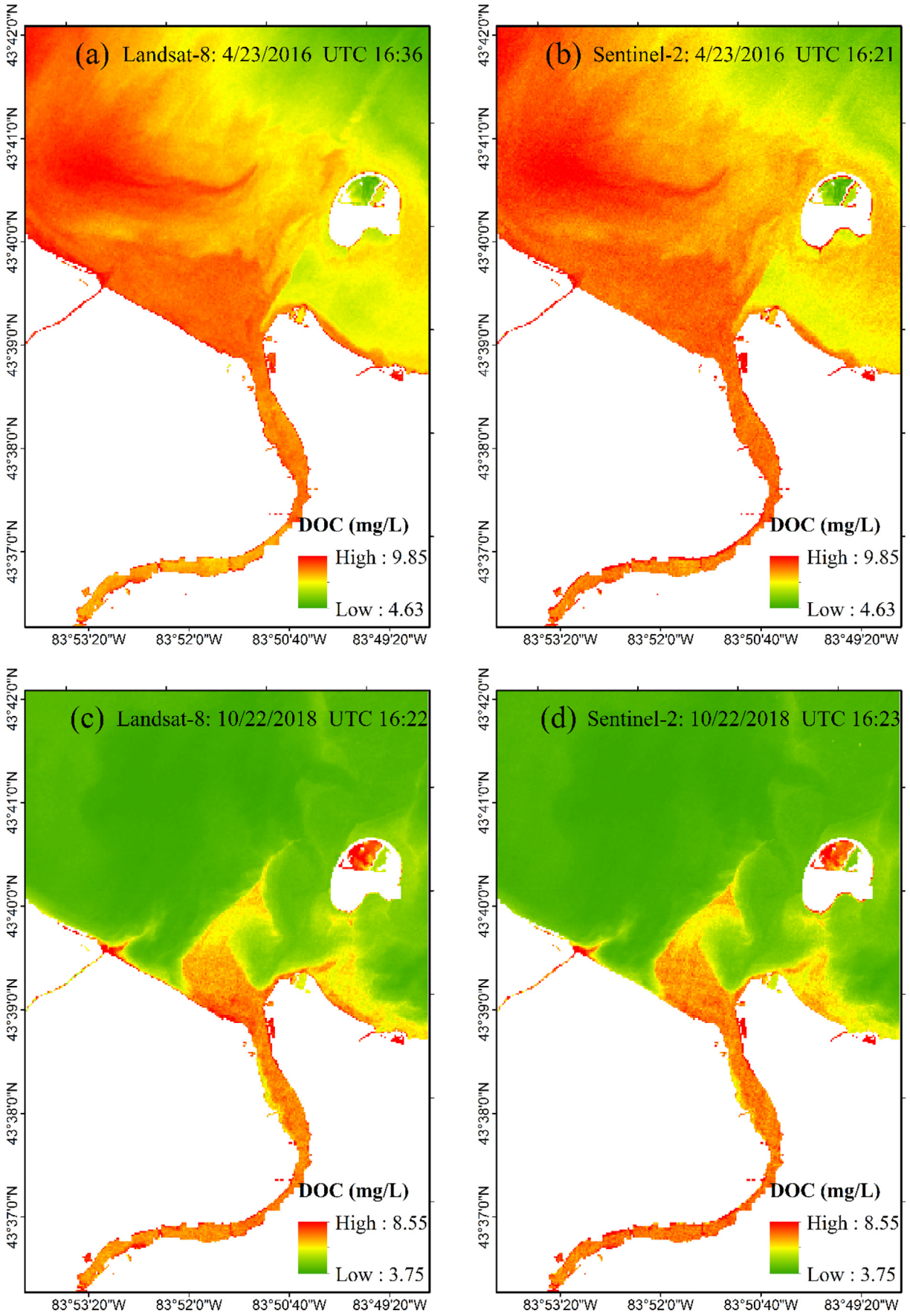

Fig. 7. Comparison between Landsat-8 and Sentinel-2 estimated DOC: (a) Landsat-8, April 23, 2016, (b) Sentinel-2, April 23, 2016, (c) Landsat-8, October 22, 2018, and (d) Sentinel-2, October 22, 2018.

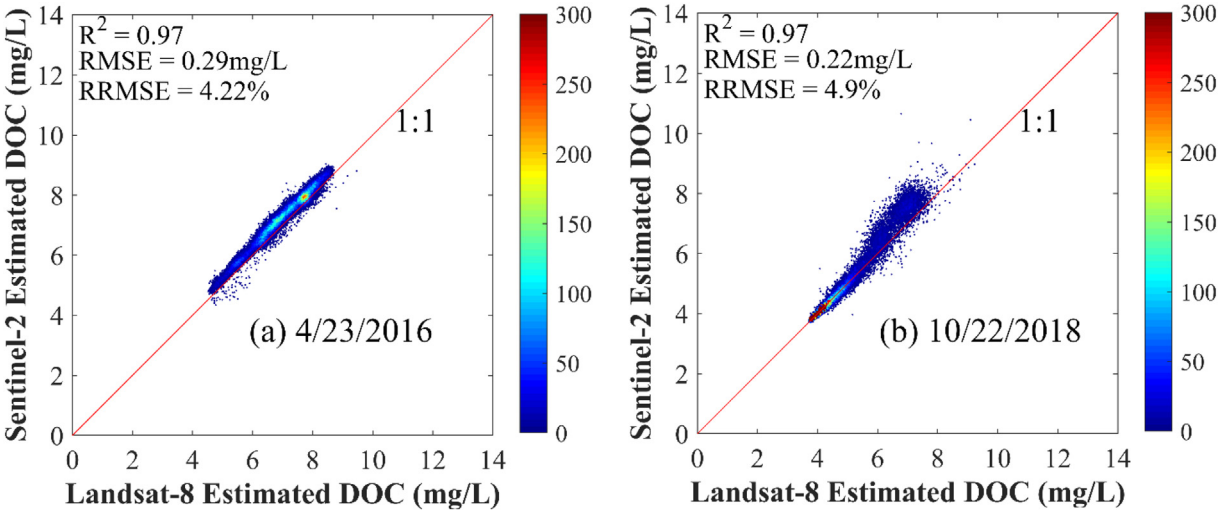

Fig. 8. Validation of Sentinel-2 DOC model using the Landsat-8 DOC model for the satellite images acquired at the same day: (a) April 23, 2016, and (b) October 22, 2018. The color bar indicates the density of the image-acquired samples.

2018a; Chen et al., 2019; Echavarría-Caballero et al., 2019; Kuhn et al., 2019; Gomes et al., 2020). Therefore, we believe that during the 6 days, the CDOM and DOC in the study site would not experience significant change. The Landsat-8 image-derived DOC was validated by the 13 samples measured on May 7, 2013, and the results (Fig. 6) show that the model performed well with RSME = 1.52 mg/L and RRMSE = 18.74%. Among the 13 samples, DOC in 11 samples was accurately derived except in samples No.5 and No.6. The two samples were located in Kawkawlin River's mouth where the discharge plume region were small and might be significantly and frequently changed by the currents in Lake Huron (Chen et al., 2017a). We found that except sample No.5 and No.6, the other samples were slightly overestimated by 11.69%. These overestimations may be caused by the gap (6 days) between the field measurement and image acquisition dates. We checked the real discharge of Saginaw River on May 1 and May 7, 2013 and found that the discharge on May 1 was slightly larger than that on May 7. It is known that there are positive correlations between river discharge and DOC/CDOM concentrations (Griffin et al., 2011; Zhu et al., 2013; Griffin et al., 2018a; Li et al., 2018; Liu et al., 2019). Therefore, although there were overestimations of Landsat-8 on May 1 compared to the field measured values on May 7, they might be reduced if compared to the true field values measured on May 1.

Because the dates of available Sentinel-2 images do not match or close to any date of our field measurement, the performance of Sentinel-2 DOC model cannot be directly examined, but it can be validated using the Landsat-8's derived results as the ground truth, just like some previous studies have done (Wu et al., 2013). In this study, there were twice that Landsat-8 and Sentinel-2 sensed the study area on the same day, i.e., on April 23, 2016 and October 22, 2018, and even at the same time (the time intervals were 15 min and 1 min, respectively), so the acquired images were used for assessing the performance of the Sentinel-2 DOC model as well as the consistency of the Landsat-8 and Sentinel-2 DOC models.

Table 1
The number of high-quality available Landsat-8 and Sentinel-2 images from 2013 to 2018.

Year	Landsat-8	Sentinel-2	Sum
2013	7	n/a	7
2014	3	n/a	3
2015	6	2	8
2016	9	5	14
2017	7	6	13
2018	6	23	29

The Fig. 7 shows the image-derived DOC from the four Landsat-8 and Sentinel-2 images acquired on April 23, 2016 and October 22, 2018. The resultant DOC distributions indicate that Landsat-8 and Sentinel-2 DOC models were with excellent consistent across the study site. DOC in the two days was with ranges 4.63–9.85 mg/L and 3.75–8.55 mg/L, respectively. To quantify the satellite consistency, the spatial resolution of Sentinel-2 images was reduced to as the same as the 30 m of Landsat-8, and then correlations between the results of the corresponding images can be computed. Results (Fig. 8) show that there was excellent consistency between Landsat-8 and Sentinel-2 DOC models: they were correlated with R^2 = 0.97, RMSE = 0.29 mg/L, and RRMSE = 4.22% on April 23, 2016, and R^2 = 0.97, RMSE = 0.22 mg/L, and RRMSE = 4.9% on October 22, 2018. These results indicate that the Sentinel-2 DOC model is accurate and Sentinel-2 and Landsat-8 have good consistency for DOC estimation in complex freshwater.

3.4. Image-observed seasonal variations of DOC and DOC-discharge relationship

The amount of valid Landsat-8 and Sentinel-2 images is shown in Table 1. Landsat-8 was launched on February 11, 2013 and the twin Sentinel-2 satellites (Sentinel-2A and Sentinel-2B) were launched on June 23, 2015 and March 7, 2017, and routinely obtained images with a 5-day interval since 2018. In terms of interval times of Landsat-8 (16 days) and Sentinel-2 (5 days), the observation frequency of previous Landsat-8 CDOM or DOC models would be improved by approximately 75% if combining similar Sentinel-2 models, and if new Sentinel-2 models can combine more Landsat-8 images, its observation frequency would be improved by approximately 25%. Both of the two combinations would be beneficial to our water quality monitoring. Therefore, from Table 1 we can see that, after 2018, image amount of jointly using Landsat-8 and Sentinel-2 is almost five times that of using single Landsat-8, and hence provided more frequent observations on inland water quality (Li et al., 2015).

The Fig. 9 shows the relationships between the image-derived DOC concentrations and the discharge of Saginaw River from 2013 to 2018. We can see that DOC covaried well with river discharges in different seasons. Previous studies have found that DOC/CDOM and chlorophyll-a are not covaried in the study site (Zhu et al., 2015), meaning that DOC is mainly sourced from the allochthonous rather than autochthonous matter. The land use and land cover of Saginaw River watershed are mainly for agriculture, making the major content of soil organic matter comes from the biological decay of crop residues and deciduous trees, and hence when the organics-rich soil particles were

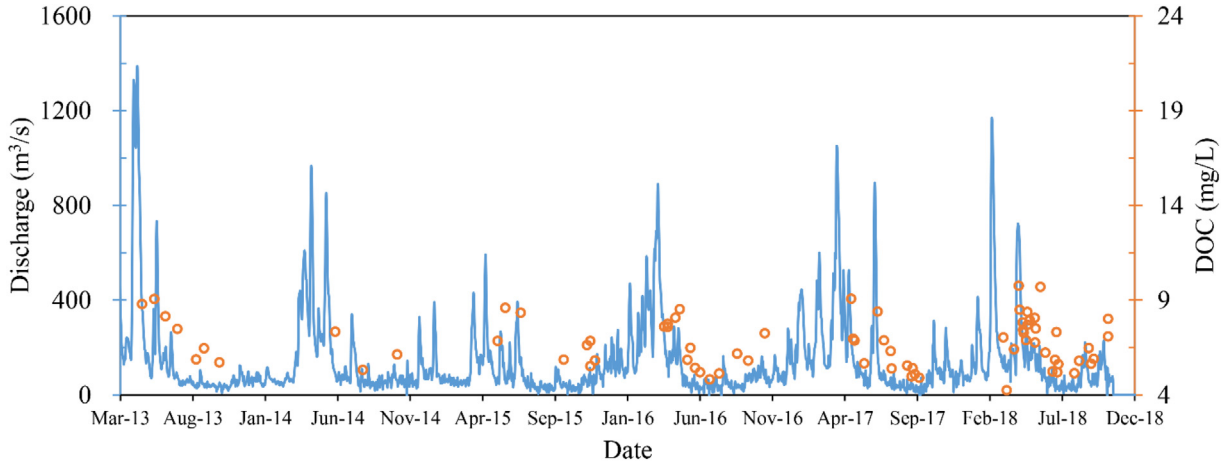

Fig. 9. DOC concentrations estimated jointly from Landsat-8 and Sentinel-2 image and the discharge of Saginaw River from 2013 to 2018.

moved into the lake by runoff and river discharge, the observed lake DOC concentrations were correspondingly increased (Griffin et al., 2011; Joshi and D'Sa, 2015; Chen et al., 2018; Li et al., 2018; Liu et al., 2019). Our results clearly show that the DOC-discharge coupling also frequently occurred in Saginaw River plume regions of Lake Huron, where DOC experiences periodically three seasonal patterns (Fig. 9):

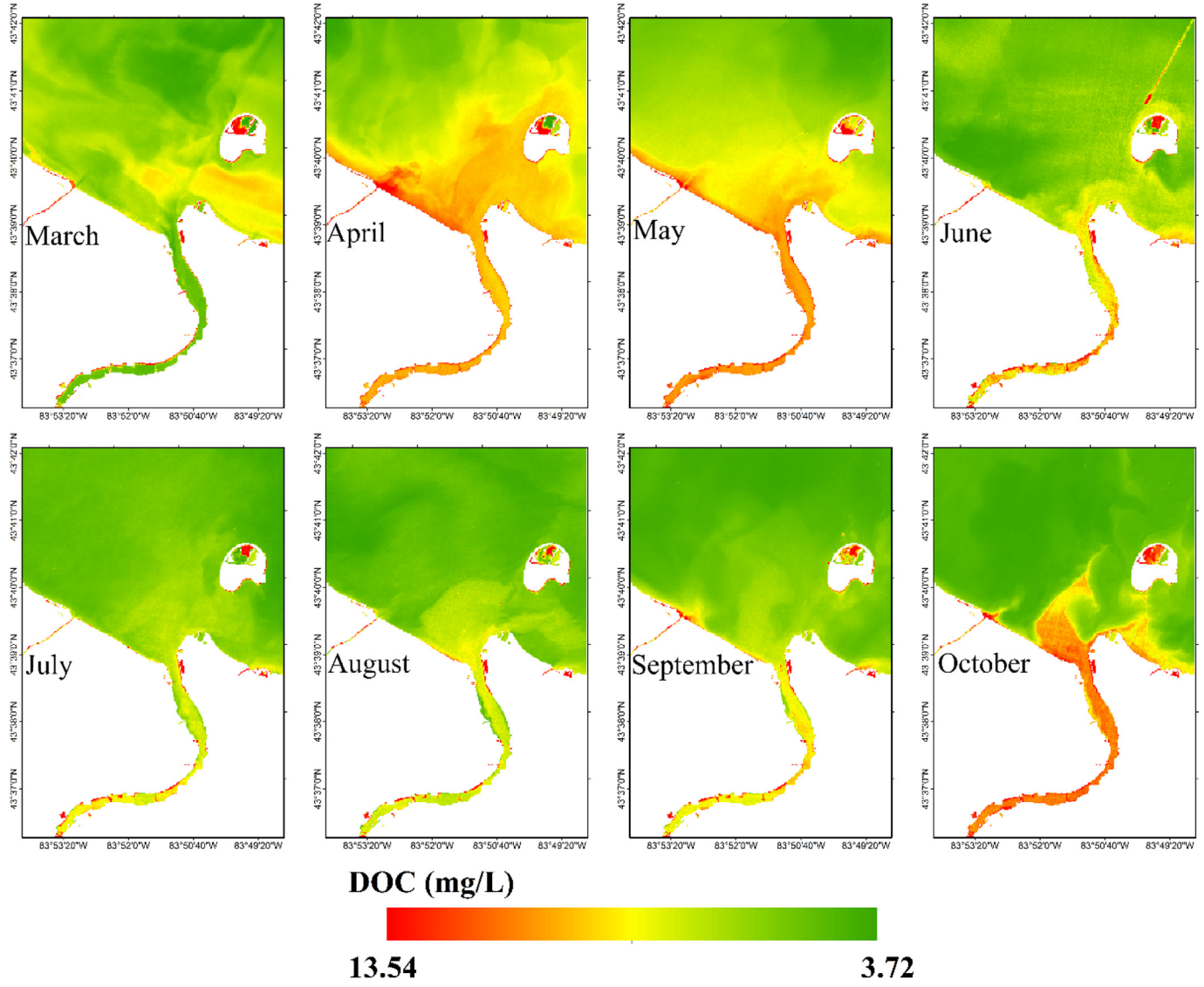

Fig. 10. Spatial distributions of monthly mean DOC in Saginaw plume regions of Lake Huron in 2018 by combining Landsat-8 and Sentinel-2 images.

(1) DOC concentrations were high from April to May; (2) then it became lower from June to August; and (3) compared with in summer, it turned to be higher again from September to November. For example, according to the image-derived results, DOC concentration was 7.6 mg/L on April 16, 2016, and changed to 4.82 mg/L in July and 7.25 mg/L in November of that year.

3.5. Monthly variations of DOC and its driving forces

We particularly mapped and analyzed the DOC variations in 2018, because the monthly observation frequency in 2018, provided by Landsat-8 and Sentinel-2 together, was the highest in the past five years. The monthly DOC image-observed distributions in Saginaw plume regions of Lake Huron, from March to October in 2018, are shown in Fig. 10. The similar three seasonal patterns also happened in 2018, see Fig. 10, in that year, the highest DOC concentration (8.63 mg/L) was found in April, while the lowest 5.82 mg/L was found in July (Fig. 11). In Saginaw Bay area, the above three seasonal patterns correspond to its climate periodicity and phenological synchrony. In spring (Apr.–May), the increased surface runoff due to snow-melting and rainfall exports large amounts of organic matter from the land to Saginaw Bay, lifting DOC concentrations in the lake. In contrast, DOC becomes lower in summer since microbial decomposition and photobleaching are enhanced as temperature and solar radiation come to be high, and in addition, the river discharge also becomes lower in summer (Del Vecchio and Blough, 2004). During the autumn and after the harvest, the crop residues and shed leaves gradually decay and lead to relatively high soil organic matter contents (Kalbitz and Kaiser, 2008). Moreover, solar radiation and water temperature drop down in autumn, causing the sink of DOC being at a low rate (Hudson et al., 2003) so that DOC concentrations become higher again.

Spatially, DOC concentrations were higher in estuarine and lakeshore regions than in the open area of Saginaw Bay. The DOC-rich water in these regions were caused by the discharge of Saginaw River and Kawkawlin River, and we also found some small DOC sources in lakeshore regions which were caused directly by human activities, such as a small plume region at latitude 43.64° and longitude −83.82°, where the DOC-rich water were made by the nearby coal-fired power plant, the Consumers Energy–D.E. Karn/J.C. Weadock Generating Complex. Along the Saginaw River to the inner bay, DOC declined in all seasons (Fig. 12). The highest DOC concentration difference between the estuary and inner Bay occurred in October

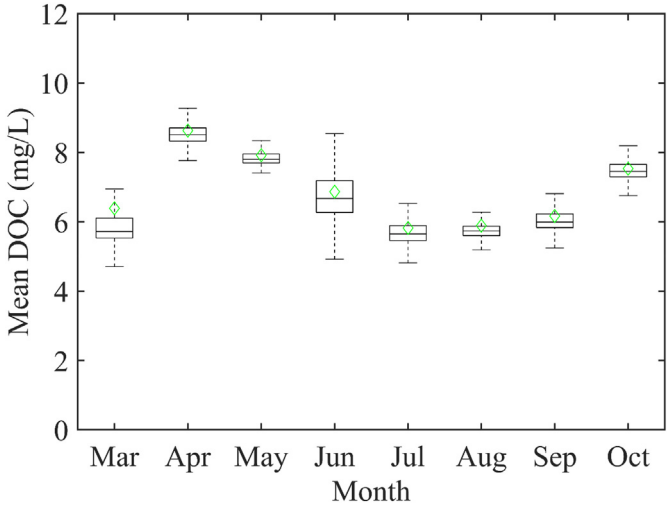

Fig. 11. Monthly mean DOC concentrations of Saginaw River in 2018. Note that the boxplot shows the minimal, median, mean (green diamond symbols), maximal, 25th and 75th percentile of DOC concentration. (For interpretation of the references to color in this figure legend, the reader is referred to the web version of this article.)

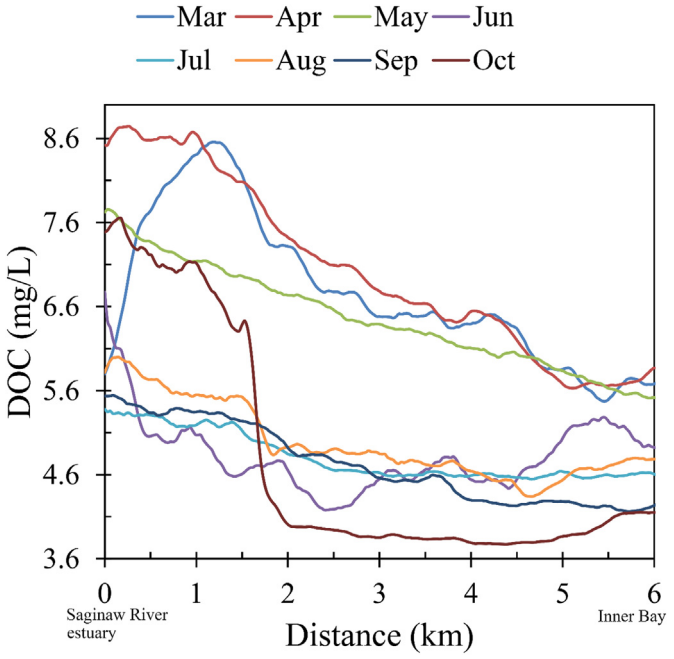

Fig. 12. Monthly mean DOC concentrations in 2018 along the Saginaw River estuary into the inner Saginaw Bay.

(7.65 mg/L versus 3.78 mg/L), while the smallest was found in July (5.33 mg/L versus 4.74 mg/L).

The Pearson correlation analysis between monthly mean DOC concentrations in Saginaw River plume regions and monthly mean discharge of Saginaw River were performed, see results in Fig. 13. They were positively correlated with $r = 0.82$ (Fig. 13(a)). The remote sensing observed DOC-discharge relationship is consistent with the long-term field observed cases in North America and Landsat-5/7 observations in high-latitude and Arctic regions (Correll et al., 2001; Griffin et al., 2011; Griffin et al., 2018a). Correll et al. (2001) sampled field organic matter in eight small watersheds on the Atlantic Coastal Plain and analyzed the effects of water discharge and land use on organic carbon, and they found that DOC was positively related with the instantaneous water discharge, but their observed correlation ($r = 0.58$, N = 219, $p < 0.00001$) is weaker than the remote sensing observation in our study site ($r = 0.82$). The stronger DOC-discharge relationships in Saginaw River watershed is reasonable because they found that TOC (total organic carbon) fluxes were more variable with precipitation in first order watershed (Correll et al., 2001), while in our study, DOC-discharge relationship could be a good proxy of TOC-precipitation relationship, and Saginaw River watershed is also a type of first order watershed dominated by the cropland. We also analyzed the relationship between DOC concentration and water temperature (WT), because microbial decomposition process of organic matter is influenced by environmental temperature, and typically, the increased temperature would lead to a decreased trend of DOC concentration (Hudson et al., 2003). Our results show there were negative correlations between WT and DOC ($r = -0.6$) but Correll et al. (2001) found that there were no significant regressions for air temperature (AT) versus TOC concentrations for spring, fall, and annual periods, but for summer and winter, the AT-TOC showed significant positive correlations ($r = 0.44$–0.65). Compared to air temperature, water temperature is more tightly and directly connected to the dissolved organic matter. Therefore, possibly our results are more accurate than the Correll's, that is, temperature, either WT or AT, is negatively rather than positively correlated to DOC concentrations. Other studies also found that AT-DOC was negatively correlated (Liu et al., 2019). However, because warmer temperatures

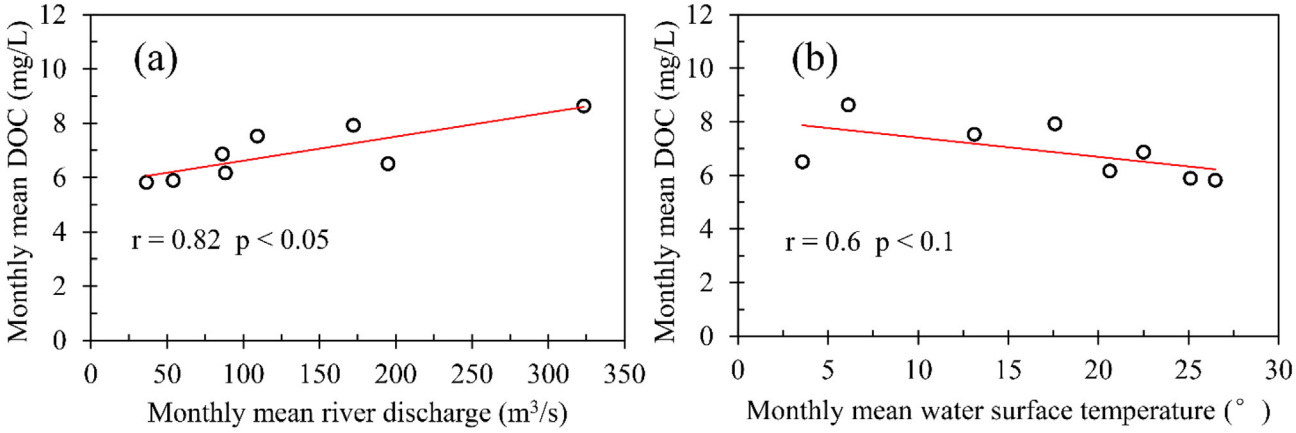

Fig. 13. Relationships between monthly mean DOC and (a) monthly mean river discharge, and (b) monthly mean water temperature.

may be stimulating DOC production and/or consumption rates by influencing microbial activity, the temperature-DOC correlations in different watersheds may hence varied and the real correlations might be too complex to be simply expressed in linear regressions.

4. Conclusion

In this study, Landsat-8 and Sentinel-2 satellites were jointly used to estimate DOC spatiotemporal variation in Saginaw Bay of Lake Huron. The field measured DOC and CDOM in the study area were with good correlation. Based on this DOC-CDOM correlation, DOC can be estimated using the known CDOM remote sensing models in study site. The DOC Landsat-8 model performed well with accuracy $R^2 = 0.86$, RMSE = 1.13 mg/L, and RRMSE = 16.28%, and DOC Sentinel-2 model were with accuracy $R^2 = 0.78$, RMSE = 1.41 mg/L, and RRMSE = 20.32%. There was high consistency between Landsat-8 and Sentinel-2 DOC models when they were applied in images acquired at the same day, the resultant $R^2 = 0.97$ and RMSE = 0.22 mg/L. The DOC concentrations jointly derived from 5-year (2013–2018) time-series Landsat-8 and Sentinel-2 images shows highly temporal variations. Satellite observation frequency in 2018 is highest across the 5-year. Furthermore, monthly mean DOC concentrations in 2018 were mapped and analyzed. Especially DOC had a significant seasonal covariation with the discharge ($r = 0.82$). DOC concentrations were relatively higher in spring, lower in summer, and higher again in autumn. These seasonal DOC changes are associated with the snow-melting, rainfall, crop harvest, defoliation, and other terrestrial and hydrological events. Besides, DOC concentrations in Saginaw Bay highly influenced by surrounding terrestrial showed significant spatial heterogeneity. We also found that DOC and water temperature had a weak negative correlation ($r = -0.6$). This study demonstrated that combining Landsat-8 and Sentinel-2 can provide accurate and frequent observations for DOC dynamics in complex inland water.

Declaration of competing interest

The authors declare that they have no known competing financial interests or personal relationships that could have appeared to influence the work reported in this paper.

Acknowledgement

We thank the USGS and ESA for providing Landsat-8, Sentinel-2 images and their processing tools. This study is supported by the National Natural Science Foundation of China (No. 41971373 and 41876031), and the National Science Foundation of USA (No. 1025547 and 1230261).

References

Alcântara, E., Bernardo, N., Watanabe, F., Rodrigues, T., Rotta, L., Carmo, A., Shimabukuro, M., Gonçalves, S., Imai, N., 2016. Estimating the CDOM absorption coefficient in tropical inland waters using OLI/Landsat-8 images. Remote Sensing Letters 7 (7), 661–670.

Bauer, J.E., Wei-Jun, C., Raymond, P.A., Bianchi, T.S., Hopkinson, C.S., Regnier, P.A.G., 2013. The changing carbon cycle of the coastal ocean. Nature 504 (7478), 61–70.

Boucher, J., Weathers, K.C., Norouzi, H., Steele, B., 2018. Assessing the effectiveness of Landsat 8 chlorophyll a retrieval algorithms for regional freshwater monitoring. Ecol. Appl. 28 (4), 1044–1054.

Bricaud, A., Morel, A., Prieur, L., 1981. Absorption by dissolved organic matter of the sea (yellow substance) in the UV and visible domains 1. Limnol. Oceanogr. 26 (1), 43–53.

Butman, D., Stackpoole, S., Stets, E., McDonald, C.P., Clow, D.W., Striegl, R.G., 2016. Aquatic carbon cycling in the conterminous United States and implications for terrestrial carbon accounting. Proc. Natl. Acad. Sci. 113 (1), 58–63.

Cao, F., Miller, W.L., 2015. A new algorithm to retrieve chromophoric dissolved organic matter (CDOM) absorption spectra in the UV from ocean color. Journal of Geophysical Research: Oceans 120 (1), 496–516.

Cao, F., Tzortziou, M., Hu, C., Mannino, A., Fichot, C.G., Del Vecchio, R., Najjar, R.G., Novak, M., 2018. Remote sensing retrievals of colored dissolved organic matter and dissolved organic carbon dynamics in North American estuaries and their margins. Remote Sens. Environ. 205, 151–165.

Cardille, J.A., Leguet, J.-B., del Giorgio, P., 2013. Remote sensing of lake CDOM using noncontemporaneous field data. Can. J. Remote. Sens. 39 (2), 118–126.

Casal, G., Monteys, X., Hedley, J., Harris, P., Cahalane, C., McCarthy, T., 2019. Assessment of empirical algorithms for bathymetry extraction using Sentinel-2 data. Int. J. Remote Sens. 40 (8), 2855–2879.

Chen, J., Zhu, W.-N., Tian, Y.Q., Yu, Q., 2017a. Estimation of colored dissolved organic matter from Landsat-8 imagery for complex inland water: case study of Lake Huron. IEEE Trans. Geosci. Remote Sens. 55 (4), 2201–2212.

Chen, J., Zhu, W., Tian, Y.Q., Yu, Q., Zheng, Y., Huang, L., 2017. Remote estimation of colored dissolved organic matter and chlorophyll-a in Lake Huron using Sentinel-2 measurements. J. Appl. Remote. Sens. 11 (3), 036007.

Chen, J., Zhu, W., Zheng, Y., Tian, Y.Q., Yu, Q., 2018. Monitoring seasonal variations of colored dissolved organic matter for the Saginaw River based on Landsat-8 data. Water Supply 19 (1), 274–281 ws2018077.

Chen, J., Zhu, W., Pang, S., Cheng, Q., 2019. Applicability evaluation of Landsat-8 for estimating low concentration colored dissolved organic matter in inland water. Geocarto International 1–15.

Cherukuru, N., Ford, P.W., Matear, R.J., Oubelkheir, K., Clementson, L.A., Suber, K., Steven, A.D.L., 2016. Estimating dissolved organic carbon concentration in turbid coastal waters using optical remote sensing observations. Int. J. Appl. Earth Obs. Geoinf. 52, 149–154.

Coble, P.G., 1996. Characterization of marine and terrestrial DOM in seawater using excitation-emission matrix spectroscopy. Mar. Chem. 51 (4), 325–346.

Coble, P.G., 2007. Marine optical biogeochemistry: the chemistry of ocean color. Chem. Rev. 107 (2), 402–418.

Cole, J.J., Prairie, Y.T., Caraco, N.F., McDowell, W.H., Tranvik, L.J., Striegl, R.G., Duarte, C.M., Kortelainen, P., Downing, J.A., Middelburg, J.J., Melack, J., 2007. Plumbing the global carbon cycle: integrating inland waters into the terrestrial carbon budget. Ecosystems 10 (1), 172–185.

Correll, D.L., Jordan, T.E., Weller, D.E., 2001. Effects of precipitation, air temperature, and land use on organic carbon discharges from Rhode River watersheds. Water Air Soil Pollut. 128 (1–2), 139–159.

Del Vecchio, R., Blough, N.V., 2004. Spatial and seasonal distribution of chromophoric dissolved organic matter and dissolved organic carbon in the Middle Atlantic Bight. Mar. Chem. 89 (1–4), 169–187.

Echavarría-Caballero, C., Domínguez-Gómez, J.A., González-García, C., García-García, M.J., 2019. Assessment of Landsat 5 images atmospherically corrected with LEDAPS in water quality time series. Can. J. Remote. Sens. 1–16.

Findley, W.G., 2003. Aquatic Ecosystems: Interactivity of Dissolved Organic Matter. Academic Press.
Godin, P., Macdonald, R.W., Kuzyk, Z.Z.A., Goñi, M.A., Stern, G.A., 2017. Organic matter compositions of rivers draining into Hudson Bay: present-day trends and potential as recorders of future climate change. Journal of Geophysical Research: Biogeosciences 122 (7), 1848–1869.
Gomes, A.C., Alcântara, E., Rodrigues, T., Bernardo, N., 2020. Satellite estimates of euphotic zone and Secchi disk depths in a colored dissolved organic matter-dominated inland water. Ecol. Indic. 110, 105848.
Griffin, C.G., Frey, K.E., Rogan, J., Holmes, R.M., 2011. Spatial and interannual variability of dissolved organic matter in the Kolyma River, East Siberia, observed using satellite imagery. J. Geophys. Res. 116 (G3).
Griffin, C., McClelland, J., Frey, K., Fiske, G., Holmes, R., 2018a. Quantifying CDOM and DOC in major Arctic rivers during ice-free conditions using Landsat TM and ETM+ data. Remote Sens. Environ. 209, 395–409.
Griffin, C.G., Finlay, J.C., Brezonik, P.L., Olmanson, L., Hozalski, R.M., 2018b. Limitations on using CDOM as a proxy for DOC in temperate lakes. Water Res. 144, 719–727.
Gurlin, D., Gitelson, A.A., Moses, W.J., 2011. Remote estimation of chl-a concentration in turbid productive waters—return to a simple two-band NIR-red model? Remote Sens. Environ. 115 (12), 3479–3490.
Huang, W., Chen, R.F., 2009. Sources and transformations of chromophoric dissolved organic matter in the Neponset River Watershed. J. Geophys. Res. 114.
Hudson, J.J., Dillon, P.J., Somers, K.M., 2003. Long-term patterns in dissolved organic carbon in boreal lakes: the role of incident radiation, precipitation, air temperature, southern oscillation and acid deposition.
Joshi, I., D'Sa, E., 2015. Seasonal variation of colored dissolved organic matter in Barataria Bay, Louisiana, using combined Landsat and field data. Remote Sens. 7 (9), 12478–12502.
Kalbitz, K., Kaiser, K., 2008. Contribution of dissolved organic matter to carbon storage in forest mineral soils. J. Plant Nutr. Soil Sci. 171 (1), 52–60.
Kirk, J.T., 1994. Light and Photosynthesis in Aquatic Ecosystems. Cambridge university press.
Kuhn, C., de Matos Valerio, A., Ward, N., Loken, L., Sawakuchi, H.O., Kampel, M., Richey, J., Stadler, P., Crawford, J., Striegl, R., Vermote, E., Pahlevan, N., Butman, D., 2019. Performance of Landsat-8 and Sentinel-2 surface reflectance products for river remote sensing retrievals of chlorophyll-a and turbidity. Remote Sens. Environ. 224, 104–118.
Kutser, T., 2012. The possibility of using the Landsat image archive for monitoring long time trends in coloured dissolved organic matter concentration in lake waters. Remote Sens. Environ. 123, 334–338.
Kutser, T., Verpoorter, C., Paavel, B., Tranvik, L.J., 2015. Estimating lake carbon fractions from remote sensing data. Remote Sens. Environ. 157, 138–146.
Lee, Z., Shang, S., Qi, L., Yan, J., Lin, G., 2016. A semi-analytical scheme to estimate Secchi-disk depth from Landsat-8 measurements. Remote Sens. Environ. 177, 101–106.
Li, J., Roy, D.P., 2017. A global analysis of sentinel-2A, sentinel-2B and Landsat-8 data revisit intervals and implications for terrestrial monitoring. Remote Sens. 9 (9), 902.
Li, J., Chen, X., Tian, L., Ding, J., Song, Q., Yu, Z., 2015. On the consistency of HJ-1A CCD1 and Terra/MODIS measurements for improved spatio-temporal monitoring of inland water: a case in Poyang Lake. Remote Sensing Letters 6 (5), 351–359.
Li, Y., Zhang, Y., Shi, K., Zhou, Y., Zhang, Y., Liu, X., Guo, Y., 2017. Spatiotemporal dynamics of chlorophyll-a in a large reservoir as derived from Landsat 8 OLI data: understanding its driving and restrictive factors. Environ. Sci. Pollut. Res. Int. 25 (2), 1359–1374.
Li, Y., Zhang, Y., Shi, K., Zhu, G., Zhou, Y., Zhang, Y., Guo, Y., 2017b. Monitoring spatiotemporal variations in nutrients in a large drinking water reservoir and their relationships with hydrological and meteorological conditions based on Landsat 8 imagery. Sci. Total Environ. 599–600, 1705–1717.
Li, J., Yu, Q., Tian, Y.Q., Becker, B.L., Siqueira, P., Torbick, N., 2018. Spatio-temporal variations of CDOM in shallow inland waters from a semi-analytical inversion of Landsat-8. Remote Sens. Environ. 218, 189–200.
Liu, B., D'Sa, E.J., Joshi, I., 2019. Multi-decadal trends and influences on dissolved organic carbon distribution in the Barataria Basin, Louisiana from in-situ and Landsat/MODIS observations. Remote Sens. Environ. 228, 183–202.
Luis, K.M., Rheuban, J.E., Kavanaugh, M.T., Glover, D.M., Wei, J., Lee, Z., Doney, S.C., 2019. Capturing coastal water clarity variability with Landsat 8. Mar. Pollut. Bull. 145, 96–104.
Miller, W.L., Moran, M.A., 1997. Interaction of photochemical and microbial processes in the degradation of refractory dissolved organic matter from a coastal marine environment. Limnology & Oceanography 42 (6), 1317–1324.
Mobley, C.D., 1999. Estimation of the remote-sensing reflectance from above-surface measurements. Appl. Opt. 38 (36), 7442.
Montanher, O.C., Novo, E.M.L.M., Barbosa, C.C.F., Rennó, C.D., Silva, T.S.F., 2014. Empirical models for estimating the suspended sediment concentration in Amazonian white water rivers using Landsat 5/TM. Int. J. Appl. Earth Obs. Geoinf. 29, 67–77.
Mouw, C.B., Greb, S., Aurin, D., DiGiacomo, P.M., Lee, Z., Twardowski, M., Binding, C., Hu, C., Ma, R., Moore, T., 2015. Aquatic color radiometry remote sensing of coastal and inland waters: challenges and recommendations for future satellite missions. Remote Sens. Environ. 160, 15–30.
Olmanson, L.G., Brezonik, P.L., Finlay, J.C., Bauer, M.E., 2016. Comparison of Landsat 8 and Landsat 7 for regional measurements of CDOM and water clarity in lakes. Remote Sens. Environ. 185, 119–128.
Pacheco, F.S., Roland, F., Downing, J.A., 2014. Eutrophication reverses whole-lake carbon budgets. Inland Waters 4 (1), 41–48.
Palmer, S.C., Kutser, T., Hunter, P.D., 2015. Remote sensing of inland waters: challenges, progress and future directions. Remote Sens. Environ. 157, 1–8.
Pan, D., Liu, Q., Bai, Y., 2014. Review and suggestions for estimating particulate organic carbon and dissolved organic carbon inventories in the ocean using remote sensing data. Acta Oceanol. Sin. 33 (1), 1–10.
Qiu, Z., Xiao, C., Perrie, W., Sun, D., Wang, S., Shen, H., Yang, D., He, Y., 2016. Using Landsat 8 data to estimate suspended particulate matter in the Yellow River estuary. Journal of Geophysical Research: Oceans 122 (1), 276–290.
Ren, J., Zheng, Z., Li, Y., Lv, G., Wang, Q., Lyu, H., Huang, C., Liu, G., Du, C., Mu, M., 2018. Remote observation of water clarity patterns in Three Gorges Reservoir and Dongting Lake of China and their probable linkage to the Three Gorges Dam based on Landsat 8 imagery. Sci. Total Environ. 625, 1554–1566.
Shuchman, R.A., Leshkevich, G., Sayers, M.J., Johengen, T.H., Brooks, C.N., Pozdnyakov, D., 2013. An algorithm to retrieve chlorophyll, dissolved organic carbon, and suspended minerals from Great Lakes satellite data. J. Great Lakes Res. 39, 14–33.
Siegenthaler, U., Sarmiento, J.L., 1993. Atmospheric carbon dioxide and the ocean. Nature 365 (6442), 119.
Slonecker, E.T., Jones, D.K., Pellerin, B.A., 2016. The new Landsat 8 potential for remote sensing of colored dissolved organic matter (CDOM). Mar. Pollut. Bull. 107 (2), 518–527.
Sòria-Perpinyà, X., Vicente, E., Urrego, P., Pereira-Sandoval, M., Ruíz-Verdú, A., Delegido, J., Soria, J.M., Moreno, J., 2020. Remote sensing of cyanobacterial blooms in a hypertrophic lagoon (Albufera of València, Eastern Iberian Peninsula) using multitemporal Sentinel-2 images. Sci. Total Environ. 698, 134305.
Sun, D., Hu, C., Qiu, Z., Shi, K., 2015. Estimating phycocyanin pigment concentration in productive inland waters using Landsat measurements: a case study in Lake Dianchi. Opt. Express 23 (3), 3055–3074.
Tebbs, E.J., Remedios, J.J., Harper, D.M., 2013. Remote sensing of chlorophyll-a as a measure of cyanobacterial biomass in Lake Bogoria, a hypertrophic, saline–alkaline, flamingo lake, using Landsat ETM+. Remote Sens. Environ. 135, 92–106.
Tehrani, N., D'Sa, E., Osburn, C., Bianchi, T., Schaeffer, B., 2013. Chromophoric dissolved organic matter and dissolved organic carbon from Sea-Viewing Wide Field-of-View Sensor (SeaWiFS), Moderate Resolution Imaging Spectroradiometer (MODIS) and MERIS sensors: case study for the Northern Gulf of Mexico. Remote Sens. 5 (3), 1439–1464.
Toming, K., Kutser, T., Laas, A., Sepp, M., Paavel, B., Nõges, T., 2016. First experiences in mapping lake water quality parameters with Sentinel-2 MSI imagery. Remote Sens. 8 (8), 640.
Tranvik, L.J., Downing, J.A., Cotner, J.B., Loiselle, S.A., Striegl, R.G., Ballatore, T.J., Dillon, P., Finlay, K., Fortino, K., Knoll, L.B., 2009. Lakes and reservoirs as regulators of carbon cycling and climate. Limnol. Oceanogr. 54 (6part2), 2298–2314.
Verpoorter, C., Kutser, T., Seekell, D.A., Tranvik, L.J., 2014. A global inventory of lakes based on high-resolution satellite imagery. Geophys. Res. Lett. 41 (18), 6396–6402.
Wu, G., Cui, L., Duan, H., Fei, T., Liu, Y., 2013. An approach for developing Landsat-5 TM-based retrieval models of suspended particulate matter concentration with the assistance of MODIS. ISPRS J. Photogramm. Remote Sens. 85, 84–92.
Xu, J., Wang, Y., Gao, D., Yan, Z., Gao, C., Wang, L., 2017. Optical properties and spatial distribution of chromophoric dissolved organic matter (CDOM) in Poyang Lake, China. J. Great Lakes Res. 43 (4), 700–709.
Xu, J., Fang, C., Gao, D., Zhang, H., Gao, C., Xu, Z., Wang, Y., 2018. Optical models for remote sensing of chromophoric dissolved organic matter (CDOM) absorption in Poyang Lake. ISPRS J. Photogramm. Remote Sens. 142, 124–136.
Zhang, Y., Zhang, Y., Shi, K., Zha, Y., Zhou, Y., Liu, M., 2016. A Landsat 8 OLI-based, semianalytical model for estimating the total suspended matter concentration in the slightly turbid Xin'anjiang Reservoir (China). IEEE Journal of Selected Topics in Applied Earth Observations and Remote Sensing 9 (1), 398–413.
Zhao, J., Cao, W., Xu, Z., Ai, B., Yang, Y., Jin, G., Wang, G., Zhou, W., Chen, Y., Chen, H., 2018. Estimating CDOM concentration in highly turbid estuarine coastal waters. Journal of Geophysical Research: Oceans 123 (8), 5856–5873.
Zheng, Z., Ren, J., Li, Y., Huang, C., Liu, G., Du, C., Lyu, H., 2016. Remote sensing of diffuse attenuation coefficient patterns from Landsat 8 OLI imagery of turbid inland waters: a case study of Dongting Lake. Sci. Total Environ. 573, 39–54.
Zhu, W., Yu, Q., 2013. Inversion of chromophoric dissolved organic matter from EO-1 Hyperion imagery for turbid estuarine and coastal waters. Geoscience and Remote Sensing, IEEE Transactions on 51 (6), 3286–3298.
Zhu, W., Tian, Y.Q., Yu, Q., Becker, B.L., 2013. Using Hyperion imagery to monitor the spatial and temporal distribution of colored dissolved organic matter in estuarine and coastal regions. Remote Sens. Environ. 134, 342–354.
Zhu, W., Yu, Q., Tian, Y.Q., Becker, B.L., Zheng, T., Carrick, H.J., 2014. An assessment of remote sensing algorithms for colored dissolved organic matter in complex freshwater environments. Remote Sens. Environ. 140, 766–778.
Zhu, W., Yu, Q., Tian, Y.Q., Becker, B.L., Carrick, H., 2015. Issues and potential improvement of multiband models for remotely estimating chlorophyll-a in complex inland waters. Selected Topics in Applied Earth Observations and Remote Sensing, IEEE Journal of 8 (2), 562–575.